Surface-reconstruction-induced geometries of Si clusters

Efthimios Kaxiras*
Institute for Theoretical Physics, University of California, Santa Barbara, California 93106
(Received 8 May 1997)

We discuss a generalization of the surface-reconstruction arguments for the structure of intermediate-size Si clusters, which leads to model geometries for the sizes 33, 39 (two isomers), 45 (two isomers), 49 (two isomers), 57, and 61 (two isomers). The common feature in all these models is a structure that closely resembles the most stable reconstruction of Si surfaces, surrounding a core of bulklike tetrahedrally bonded atoms. We investigate the energetics and the electronic structure of these models through first-principles density-functional theory calculations. These models may be useful in understanding experimental results on the reactivity of Si clusters and their shape as inferred from mobility measurements. [S0163-1829(97)07344-X]

I. INTRODUCTION

Silicon is a material that attracts considerable interest due to its technological importance. It has also come to be regarded as the representative covalently bonded solid. In the last decade, a new form of Si has generated much excitement because it holds promise for technological applications as well as for providing unique insight into the nature of covalently bonded materials.[1] This new form is clusters of Si, which consist of a few tens to a few hundreds of atoms and have properties different from the bulk. The properties of Si clusters depend on their size, and a detailed study of this dependence could potentially lead to a better understanding of how chemical bonding evolves from that characteristic of small molecules to that characteristic of the bulk.

Despite much theoretical and experimental work on Si clusters during the last decade, little is known about their structure. It is self-evident that for very small cluster sizes, all of the atoms in a cluster will be exterior atoms, in the sense that there is no shell formed by a subset of atoms that completely surrounds any one atom. These very small Si clusters should, therefore, be viewed as molecules, i.e., entities with unique structural, physical, and chemical characteristics that do not resemble other forms of Si. This picture was originally proposed by Phillips,[2] who analyzed early experiments on fragmentation patterns.[3,4] Equally evident is the fact that beyond a certain size there will be interior atoms completely surrounded by a shell of other exterior atoms. (In the following, we use the terms ''interior'' and ''exterior'' as defined above to characterize cluster atoms, and reserve the terms ''bulk'' and ''surface'' to characterize atoms of the solid.) It is also natural to expect that for a large enough size, the cluster will resemble a crystalline fragment.

The size at which the transition from molecules to bulklike fragments takes place has not yet been determined precisely, although several theoretical predictions have been made.[5,6] It has also been proposed that the experimentally observed sharp transition in the shape of Si clusters,[7] which occurs at around size 27, may be related to the onset of structures with interior (''bulklike'') and exterior (''surfacelike'') atoms in the cluster.[8] Such a transition in shape had actually been predicted by theoretical simulations.[9]

The structure of the small Si clusters (up to 10 atoms) has been determined by extensive theoretical calculations[10–12] and by comparison of calculations to spectroscopic measurements.[13–17] Much less is known for the larger clusters, although a number of interesting models have been proposed. One possibility is models analogous to fullerene cages,[18,19] but given the tendency of Si to form fourfold-coordinated structures this seems unlikely. A different approach is to consider models with nonspherical shapes for medium sizes[8,20,21] or with interior and exterior atoms for larger sizes.[22–24] The assumption that there exist interior and exterior atoms does not necessarily imply that their respective environment will resemble that of bulk or surface atoms. Nevertheless, it is an attractive proposition to consider what types of structures can be produced if geometries resembling the bulk structure (for interior cluster atoms) and the surface reconstructions (for exterior cluster atoms) were to dominate the cluster geometry. Only a few cluster sizes are compatible with the requirement that *all interior cluster atoms* have environments that closely resemble the bulk structure, and *all exterior cluster atoms* have environments that closely resemble surface reconstructions. We call the resulting models surface-reconstruction-induced geometries (SRIG's). This idea has been invoked as an explanation of the existence of magic numbers in Si clusters[22] as revealed by their reactivity with various chemical agents.[25–30]

In this paper, we present in Sec. II a thorough investigation of SRIG models for the structure of selected clusters spanning sizes from 33 to 61 atoms. In Sec. III we use first-principles density-functional theory calculations to study the energetics and electronic properties of these models. Finally, in Sec. IV we comment on the relevance of these models to experimental observations of the reactivity and the mobility of Si clusters.

II. SURFACE-RECONSTRUCTION-INDUCED GEOMETRIES

Based on the assumption that the surface reconstruction determines the cluster geometry, we have constructed models for Si clusters in which exterior atoms resemble closely the coordination and bonding of atoms in the most stable surface reconstructions of Si, including the (111) 7×7 dimer-adatom-stacking (DAS) fault reconstruction,[31] the

(100) 2×1 dimer reconstruction, and the (111) 2×1 π-bonded chain reconstruction.[32] All interior atoms have the coordination and bonding arrangement of bulk Si atoms, i.e., fourfold tetrahedral coordination. The special sizes for which we were able to construct such models include the sizes 33, 39, 45, 49, 57, and 61. This does not exclude the possibility of other sizes that have similar bonding arrangements in this size range. In order to construct these models we imposed two additional constraints: (i) that the clusters have an atom at their geometric center, and (ii) that the clusters have tetrahedral overall symmetry. These constraints were motivated by simplicity considerations and not from any physical requirements. If the constraints are relaxed, it might be possible to construct additional structures with similar characteristics but lower symmetry.

In describing the cluster geometries, we adopt the following conventions: We will display *only the exterior atoms* of the cluster, in a two-dimensional picture that is obtained by unfolding three of the four sides of the tetrahedron symmetrically around the fourth side. In so doing, one obtains an equilateral triangle, at the center of which there is a smaller, inverted equilateral triangle corresponding to one side of the tetrahedron around which the other three sides have been unfolded. We denote the sides of the tetrahedron by dotted lines in all the structural figures. In the models we discuss there exist one to five interior atoms, which are not shown in the structural figures. The position of these interior atoms is discussed in detail along with every structural model. What are actually shown in the structural figures are the projections of atoms on the faces of the tetrahedron. For simplicity we refer to these projections as the atomic positions. This manner of displaying the cluster geometries has the added advantage that the reader can easily construct schematic three-dimensional models of the cluster exterior by cutting out the two-dimensional figures, folding them at the three edges of the central inverted triangle, and gluing the outer edges together.

We have also adopted a shading scheme that is common to all the cluster sizes: First, we indicate by open circles (we call those white atoms) the exterior atoms that are at the apexes of the tetrahedron; there are four such atoms in each model. In some of the models (45B, 61A, 61B) there exists an additional set of four atoms at the centers of the faces of the tetrahedron, which we also denote by open circles. Next, we indicate by hatched circles the atoms that are bonded to the first set of white atoms; there are twelve such atoms in each model. Next, there are atoms that are bonded to the twelve hatched atoms, and are indicated by gray circles. Finally, there are atoms shown in black, which are bonded to the gray atoms or to the white face-center atoms, but not to the hatched or white apex atoms. Sets of atoms with the same shading are equivalent by symmetry. With these conventions, we proceed to describe the individual cluster models in detail.

We begin with the cluster of size 33, shown in Fig. 1. This cluster had been proposed previously,[22] and consists of 28 exterior atoms and 5 interior atoms. Of the five interior atoms, one is at the geometric center of the tetrahedron and the other four are bonded to the central atom in directions pointing away from the center toward the vertices of the tetrahedron. All interior atoms are fourfold coordinated as atoms in bulk Si are. The neighbors of the four interior atoms other than the central one are the twelve hatched exterior atoms. The hatched exterior atoms are also fourfold coordinated, but their bonds are at angles severely distorted relative to the tetrahedral angle. The neighbors of the hatched exterior atoms are the four interior atoms (other than the central one) and the twelve gray exterior atoms that are threefold coordinated: they have two bonds to the hatched exterior atoms and one bond to another gray exterior atom each. Finally, there are four exterior white atoms at the apexes of the tetrahedron; these atoms are three-fold coordinated, and are bonded to three hatched exterior atoms.

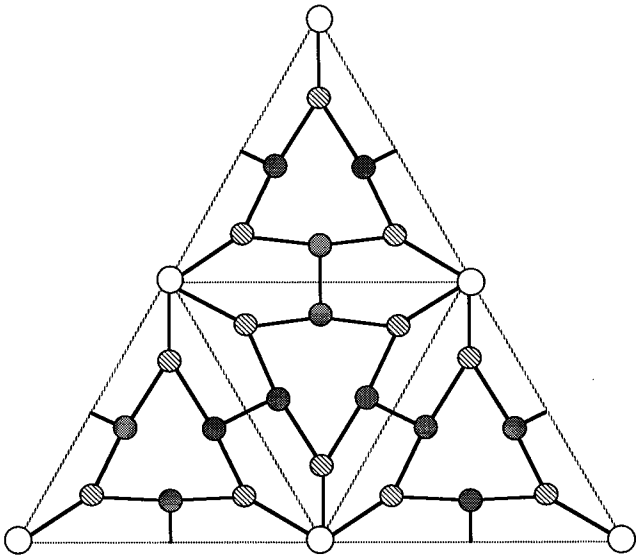

FIG. 1. Projected structure of the exterior atoms in the 33 model. Three types of atoms are shown, white apex atoms, hatched atoms, and gray atoms. The atoms of each kind are equivalent by symmetry. The four triangles outlined by dotted lines represent the four sides of a tetrahedron, unfolded around the central triangle. The darker solid lines represent covalent bonds between atoms. The five tetrahedrally bonded interior atoms are not shown.

The close similarity of this structure with surface reconstructions of Si involves two elements: (a) The four white apex atoms are in local geometries that are very similar to the adatoms on the Si(111) 7×7 reconstruction: the adatoms are directly above second layer bulk Si atoms (in the present model this role is played by the four interior atoms other than the central one). (b) The twelve gray exterior atoms are bonded in pairs like the dimers on the Si(100) 2×1 reconstruction; these atoms also play the role of the dimers that characterize the Si(111) 7×7 reconstruction and help stabilize the adatom reconstruction. Thus, in this model there is a cooperative effect that combines features from the two most stable surface reconstructions of Si to produce a highly symmetric structure with 5 interior and 28 exterior atoms.

It is noteworthy that the bonding arrangement of exterior atoms in this structure consists of pentagonal rings (with corners at one white, two hatched, and two gray atoms) and distorted hexagonal rings (they appear to be almost triangles in Fig. 1, with corners at three hatched and three gray atoms). In this sense, the shell of exterior atoms resembles the structure of the C_{28} fullerene, which has been studied exten-

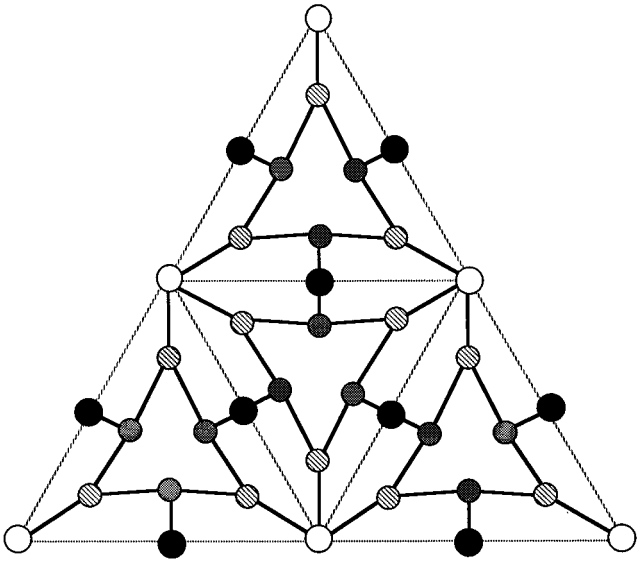

FIG. 2. Same as in previous figure, for model 39A. There are four types or atoms, white, hatched, gray, and black.

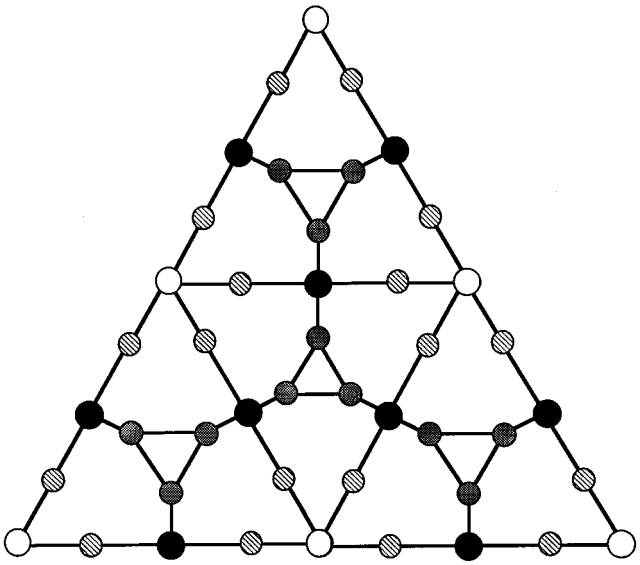

FIG. 3. Same as in previous figure, for model 39B.

sively as the smallest stable fullerene.[33–35] The resemblance, however, is superficial, since it is limited to this geometric aspect, while the C_{28} fullerene is stabilized by the π bonding of atoms at the six hexagonal rings and the Si_{33} structure is stabilized by the presence of the adatom and dimer surface features, as well as the presence of the five interior atoms. Additional important differences concern the electronic properties of the two models, with the C_{28} cluster being an open-shell structure,[35] while the Si_{33} model is a closed-shell structure (see Sec. IV).

We next consider the two models for the Si cluster with 39 atoms. The first model (referred to as 39A, shown in Fig. 2) is similar to the 33-atom model discussed above, with six additional atoms that form bonds to the gray atoms (shown as black, at the midpoints of tetrahedron edges). In this model, the white, hatched, and gray atoms are coordinated as in the 33-atom model. The six extra atoms are placed between pairs of gray atoms, and form new bonds to those atoms that become fourfold coordinated. The six extra atoms are twofold coordinated each. This type of atomic arrangement is not usually observed on Si surfaces. However, it is a reasonable arrangement for Si atoms that cannot find close neighbors to bond to. The preferred bonding for these twofold-coordinated atoms will be through p orbitals to their two neighbors, while they retain two of their four valence electrons in a low-energy nonbonding s orbital.

The second model for the 39-atom cluster (referred to as 39B, shown in Fig. 3), consists of a different geometric pattern. The four white apex atoms are in similar arrangements as in the 39A model. The hatched atoms have three bonds, one to interior atoms, one to white apex atoms and one to black atoms at the centers of the tetrahedron edges. The gray atoms no longer form dimers; instead, they form trimers centered at the faces of the tetrahedron. This is a somewhat unusual arrangement for Si atoms, and is not encountered in native surface reconstructions of Si, since the presence of trimer units induces significant strain on the surface. However, a trimer reconstruction of this type is common for group-V atoms on the surfaces of III-V semiconductors,[36] or when the group-V elements are used as passivating layers on the Si(111) surface.[37] Moreover, group-IV elements like Sn and Pb also form trimer units on the Si(111) surface.[38] We suggest that under the proper conditions (represented here by the size of the cluster) similar trimer units of Si atoms may be stable on the cluster surface. Finally, there are six atoms at the centers of the edges of the tetrahedron, which in this model are fourfold coordinated with two bonds to the hatched atoms and two more bonds to gray atoms in the trimers. This arrangement results in threefold and sevenfold rings on the exterior shell of the cluster and is markedly different from the previous geometry for size 39.

The first model we considered for the 45-atom cluster (referred to as 45A, shown in Fig. 4) is a simple variation of the 39B model: the trimers at the centers of the tetrahedron

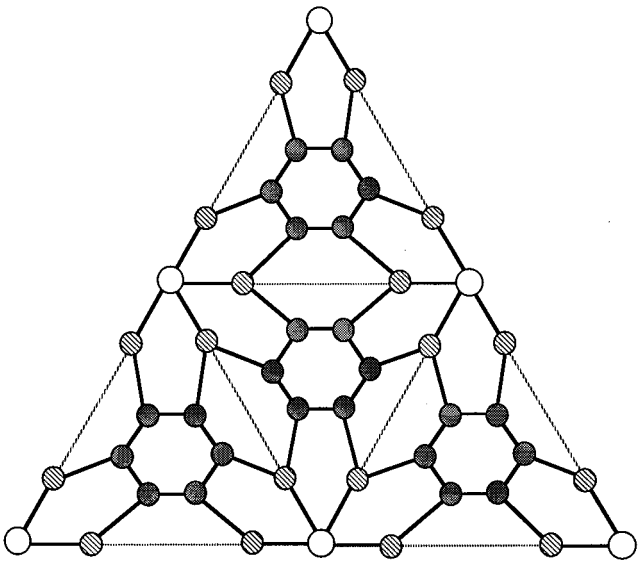

FIG. 4. Same as in previous figure, for model 45A. Three types of atoms are shown, white, hatched, and gray.

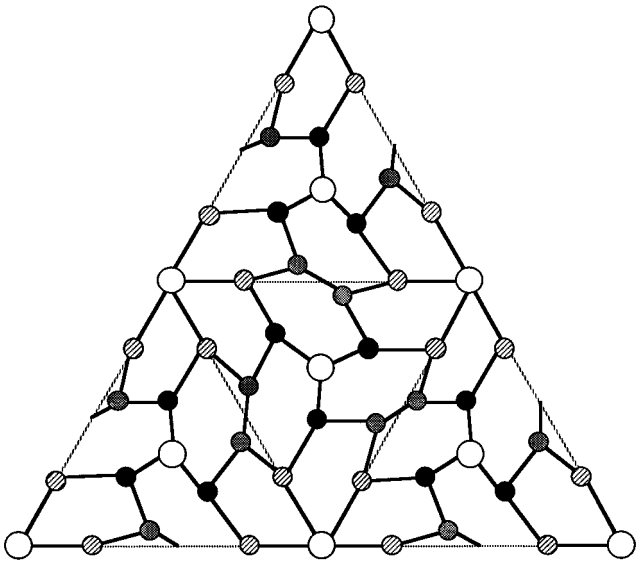

FIG. 5. Same as in previous figure, for model 45B. The chirality of this model is evident in the zig-zag chains of atoms that straddle the dotted lines. This model also serves as the shell for the 49A and 49B models, in which the four apex white atoms or the four face-center white atoms become equivalent to adatoms on the (111) (7×7) reconstruction, by the addition of a five interior atom core.

faces are replaced by hexagons and the black atoms at the centers of the tetrahedron edges are eliminated. This should help reduce the strain induced by the trimers, and it should enhance the stability of the apex atoms: the coordination of their neighboring hatched atoms has been restored to four (one apex atom, one interior atom, and two gray atoms), while the exterior pattern again contains three pentagonal rings around each white apex atom and dimers of gray atoms. In addition to the pentagonal rings (with corners at one white apex, two hatched, and two gray atoms), the exterior of the 45A model contains two types of hexagons: one composed of six gray atoms and one composed of four gray and two hatched atoms. In this sense, the exterior of this model bears a superficial resemblance to the C_{40} fullerene structure,[24] but just like in the case of Si_{33} and its companion fullerene C_{28}, the stability and electronic properties of the two types of clusters are quite different.

The next model for a 45-atom Si cluster (45B) is illustrated in Fig. 5, and corresponds to a different type of exterior bonding arrangement.[22] In this case there is only one interior atom, bonded to the four white atoms that occupy the centers of the tetrahedron faces. The white atoms at the tetrahedron apexes are no longer at positions that resemble the adatom structure of the Si(111) 7×7 reconstruction. Instead, they form intersection points where zig-zag chains consisting of hatched and gray atoms meet. The presence of these chains should produce a low-energy exterior shell because they resemble closely the chains of atoms in the other stable reconstruction of the Si(111) surface, the π-bonded chain model proposed by Pandey.[32] In this model, the dangling bonds on the neighboring chain atoms form π-bonded combinations. The geometry of the exterior shell consists of pentagonal rings around the four white apex atoms and hexagonal rings around the four white face-center atoms. Since there is only one interior atom bonded to the four face-center white atoms, the hatched atoms are only three-fold coordinated, with all their neighbors belonging to the exterior shell. The gray and black atoms are threefold coordinated, as are the apex white atoms. The only atoms that are fourfold coordinated, other than the central atom, are the four white atoms at the centers of the tetrahedron faces. This model has chirality (i.e., there exist equivalent left- and right-handed versions), which is evident from the fact that the zig-zag chains do no lie on any high-symmetry direction of the tetrahedron, and thus break the left-right symmetry of the previous models.

The same exterior shell can be used to construct two different models for the 49-atom cluster. We refer to these models as 49A and 49B. The first (49A) consists of the exterior shell shown in Fig. 5 plus five interior atoms, one at the geometric center of the tetrahedron and four more bonded to the central atom, and pointing away from it toward the four white apex atoms. The second (49B) consists of the same exterior shell and five interior atoms again, one at the geometric center of the tetrahedron and four more bonded to the central one and pointing away from it, toward the four white atoms at the centers of the tetrahedron faces. In the case of model 49A, the four white apex atoms have a coordination similar to that of adatoms on the Si(111) 7×7 DAS reconstruction, as described in the case of the 33-atom model. In the case of model 49B, the role of adatoms is assumed by the four white atoms at the centers of the tetrahedron faces. In both cases, the atoms that are bonded to the adatoms become fourfold coordinated. Specifically, in model 49A the hatched atoms become fourfold coordinated, while in model 49B the black atoms become fourfold coordinated. Since the exterior geometry in models 49A and 49B is the same as in model 45B, the pattern of pentagons and hexagons is the same. The important difference between models 49A and 49B is that in the first the adatoms (white apex atoms) are surrounded by three pentagonal rings, while in the second the adatoms (white face-center atoms) are surrounded by three hexagonal rings.

The model for the 57-atom cluster is an extension of the 45A model, in which the sixfold rings of gray atoms on the tetrahedron faces are replaced by ninefold rings as shown in Fig. 6. This is achieved by the addition of three extra atoms (shown in black) on each tetrahedron face. The rest of the cluster structure is the same as the 45A model, with five interior atoms (one at the geometric center of the tetrahedron and four more bonded to it, pointing toward the four white apex atoms) and the four white apex and twelve hatched atoms in similar positions as before. The extra atoms that turn the face-centered hexagonal rings of the 45A model into ninefold rings, are themselves bonded in dimerlike pairs across the centers of the tetrahedron edges. In this way the exterior shell is composed of ninefold rings centered at the tetrahedron faces and two types of pentagonal rings, one with corners at a white apex, two hatched, and two gray atoms, and one with corners at a hatched, two gray, and two black atoms.

The two models we have constructed for the 61-atom cluster involve geometries that have four white face-center atoms, in two different configurations. The first configuration (labeled 61A, shown in Fig. 7) derives from the 57-atom

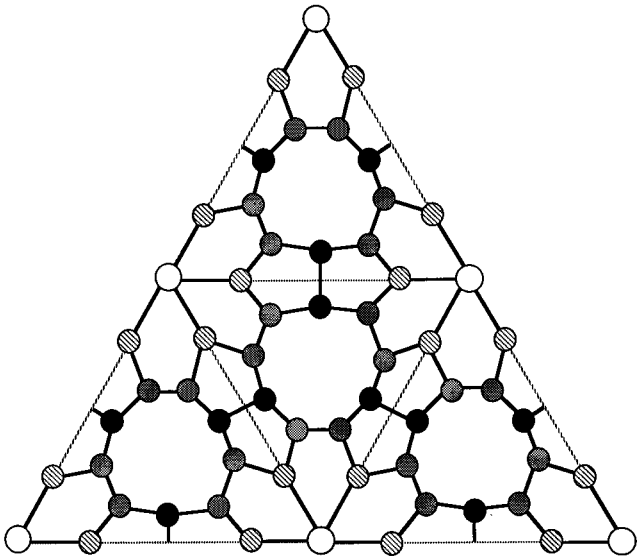

FIG. 6. Same as in previous figure, for the 57 model.

model, with the additional white atoms bonded to the three black atoms on each face, and with the dimer bonds between black atoms broken. The remaining atoms are in exactly the same configuration as in the 57-atom model. This change modifies the exterior shell, which now consists of eightfold rings (centered at the edges of the tetrahedron and composed of two hatched, four gray, and two black atoms) and two types of pentagonal rings, one composed of a white apex, two hatched, and two gray atoms, and the other composed of a white face-center, two black, and two gray atoms. In this model, as far as the exterior shell is concerned, the white apex atoms and the white face-center atoms are equivalent. Therefore the four interior atoms (other than the central one) can be considered to be pointing toward either the white apex or the white face-center atoms.

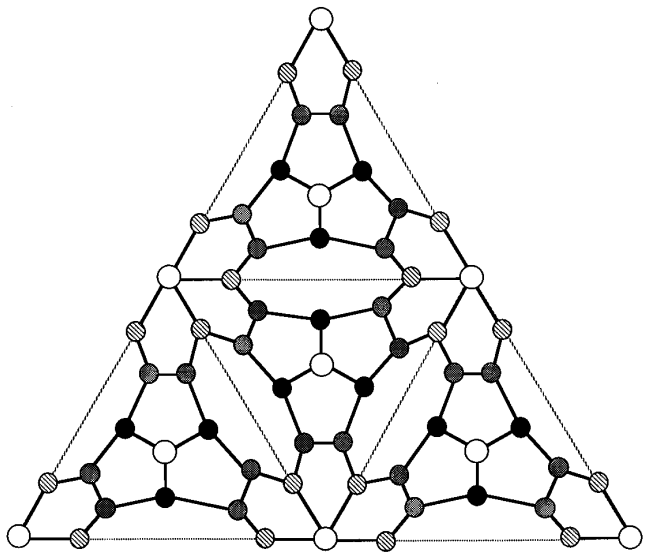

FIG. 7. Same as in previous figure, for the 61A model. Five types of atoms are shown, white apex, white face-center, hatched, gray, and black.

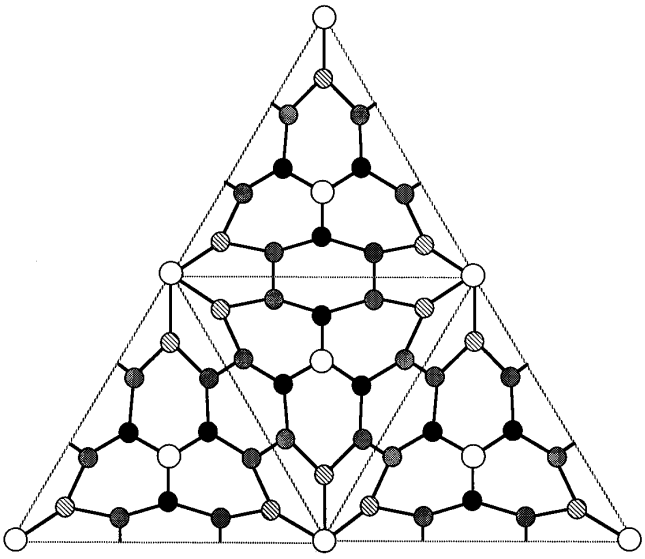

FIG. 8. Same as in previous figure, for the 61B model.

Finally, the second model for a 61-atom cluster (labeled 61B, shown in Fig. 8) contains four white apex atoms at adatom positions, surrounded by hatched atoms that form pentagonal rings with adjacent gray atoms, and four white face-center atoms that form hexagonal rings with a hatched, two gray, and two black atoms. In this case the four white apex atoms and the four white face-center atoms are not equivalent. The four interior atoms (other than the central one) are bonded to the four white apex atoms, since those have the benefit of being surrounded by pentagonal rings, which should stabilize their adatomlike features. In the 61B model, the exterior shell consists of pentagonal and hexagonal rings, which gives it a superficial resemblance to the corresponding C_{56} fullerene structure.

III. STRUCTURAL, ENERGETIC, AND ELECTRONIC FEATURES OF SRIG MODELS

Having described the geometric features of the SRIG models, we discuss next the results of energy optimization and electronic structure calculations for these models. The calculations are based on density-functional theory in the local-density approximation[39] (DFT-LDA. Although these calculations do not necessarily provide the most accurate comparisons of cluster energies, they are reasonably reliable in determining optimal geometries by minimizing the magnitude of the calculated Hellmann-Feynman forces. The present calculations employ a plane-wave basis with a cutoff energy of 8 Ry, and a cubic supercell with lattice constant equal to 15.875 Å (which gives a basis of 10 400 plane waves), for the clusters of sizes 33–49, and equal to 17.463 Å, for the clusters of sizes 57 and 61 (which gives a basis of 13 600 plane waves). With these supercells the periodic images of the clusters are reasonably well separated. A single k point (the center of the supercell Brillouin zone) was used in all the cluster calculations. The Car-Parrinello iterative scheme[40] was used to solve the Kohn-Sham equations self-consistently, and nonlocal norm-conserving pseudopotentials were employed to model the atomic cores.[41]

TABLE I. Atomic positions in a.u. of representative atoms for the optimized structures of clusters of sizes 33–61. Atoms labeled 1 are in the interior of the cluster, the rest of the atoms are on the exterior and correspond to the atoms shown in Figs. 1–8.

	33	39A	39B	45A	45B	49A	49B	57	61A	61B
1(x)	2.39471	2.38887	2.59713	2.57556	2.50590	2.48468	−2.84402	2.47912	2.64227	2.52290
1(y)	2.39471	2.38887	2.59713	2.57556	2.50590	2.48468	−2.84402	2.47912	2.64227	2.52290
1(z)	2.39471	2.38887	2.59713	2.57556	2.50590	2.48468	−2.84402	2.47912	2.64227	2.52290
2(x)	5.21249	5.16076	2.47377	2.99354	−0.11844	0.85354	1.15471	3.09986	3.16035	1.74224
2(y)	5.21249	5.16076	2.47377	2.99354	3.90217	4.39152	4.53560	3.09986	3.16035	5.59316
2(z)	0.25158	0.23991	−5.51192	7.03966	5.80660	6.28003	6.21782	6.85742	7.11649	5.59316
3(x)	1.52358	1.65023	3.39552	1.18201	1.73935	−2.03724	−1.72237	1.10146	1.13596	1.31967
3(y)	1.52358	1.50238	3.39552	4.13728	7.67793	6.86991	7.10602	4.19919	4.16677	4.34534
3(z)	−6.81708	−7.11171	6.87579	−7.15181	−4.25387	4.12951	4.35574	−7.33086	−7.16307	−8.39439
4(x)	4.97057	4.98998	6.55082	6.15942	−0.46391	−0.85430	−0.68414	−1.76564	5.29138	5.41968
4(y)	4.97057	4.98998	6.55082	6.15942	2.20720	2.05072	2.06772	1.76564	5.29138	5.41968
4(z)	4.97057	4.98998	6.55082	6.15942	9.84219	9.58102	9.29718	11.08793	−8.87922	−9.17398
5(x)		10.71204	8.16900		−5.11695	5.14767	5.30305	6.25738	6.31190	6.21939
5(y)		0.00000	0.00000		−5.11695	5.14767	5.30305	6.25738	6.31190	6.21939
5(z)		0.00000	0.00000		−5.11695	5.14767	5.30305	6.25738	6.31190	6.21939
6(x)						−5.83946	−5.61324		−8.47946	−8.50096
6(y)						−5.83946	−5.61324		−8.47946	−8.50096
6(z)						−5.83946	−5.61324		−8.47946	−8.50096

In Table I we provide a list of the atomic positions for the SRIG models. In this table only the positions of inequivalent atoms are given, with the remaining positions obtained by applying symmetry operations of the tetrahedral group. The position of the central atom in each cluster is taken to be the origin of the coordinate system and is omitted from the list of positions.

We discuss first certain structural features of the optimized cluster geometries. These considerations were motivated by some exciting recent experiments that are able to resolve aspects of the cluster geometry through gas phase mobility measurements.[42] In the simplest picture, the mobility measurements reveal the projected cross section of the cluster. For spherically shaped clusters, this cross section is given by $\Omega = \pi b_{\min}^2$, where $b_{\min}$ is the distance of closest approach between gas phase molecules and the cluster. By considering the atoms on the surface cluster as points, we can obtain $b_{\min}$ as the distance of the atom farthest from the cluster center, which gives the values of Ω tabulated in Table II. This quantity is a coarse measure of the cluster geometry and gives approximately the overall cluster size in cross section. From the comparison of Ω values in Table II, it is evident that the cluster cross section does not follow exactly the number of atoms in the cluster. It is also interesting that the clusters with the highest cohesive energy (see following paragraph and Table II) also have the smallest Ω (especially the models 33, 45A, 49A, and 49B), i.e., the lowest-energy clusters are also the most compact ones.

As Shvartsburg and Jarrold have pointed out,[44] the projection of the cluster cross section is appropriate for clusters which are locally convex. When the surface of the cluster contains concave regions, the scattering cross section is increased due to multiple collisions. In Table II we list the momentum transfer collision integrals (with He atoms, at 298 K) for the model geometries described in the present paper. These values have been evaluated by A. A. Shvartsburg[43] using the trajectory calculations method recently developed by Jarrold and co-workers.[42] The calculations have been performed by propagating the trajectories of He atoms in the cluster effective potentials, constructed as a sum of pairwise Si–He interactions plus the charge-induced dipole term with the ionic charge uniformly delocalized among all cluster atoms.[45] The comparison with the experimental values, also given in Table II as percent deviation, is revealing: for some clusters, especially the models 33, 39B, 45A, and 49A, the experimental and theoretical values are in excellent agreement (less than 2% difference), while for the clusters larger than 49 atoms the differences are much larger.

For the energetic comparisons, since the type of calculations employed here do not provide an accurate estimate of

TABLE II. Structural, energetic, and electronic features of SRIG models: Cross section $\Omega = \pi b_{\min}^2$, computed momentum transfer collision integrals ρ_{th} for the models (Ref. 43) [and their percent deviation from measured experimental values for clusters of corresponding sizes (Ref. 45)], cohesive energy per atom E_c and HOMO-LUMO gap E_g (for the clusters that have no gap, the degeneracy and filling of the partially occupied level at the Fermi energy are given in brackets).

Cluster	Ω (Å^2)	ρ_{th}	E_c (eV/atom)	E_g (eV)
33	52	2760 (−2.1%)	3.816	0.35
39A	101	3415 (+9.4%)	3.741	0.64
39B	87	3200 (+2.6%)	3.599	0.77
45A	78	3380 (−0.1%)	3.844	0.30
45B	90	3590 (+6.0%)	3.807	[2 (1/2)]
49A	86	3635 (+0.9%)	3.858	0.07
49B	81	3555 (−1.2%)	3.855	[3 (2/3)]
57	114	4185 (+6.2%)	3.712	0.04
61A	141	4460 (+8.8%)	3.800	[3 (2/3)]
61B	142	4615 (+12.6%)	3.674	[3 (1/3)]

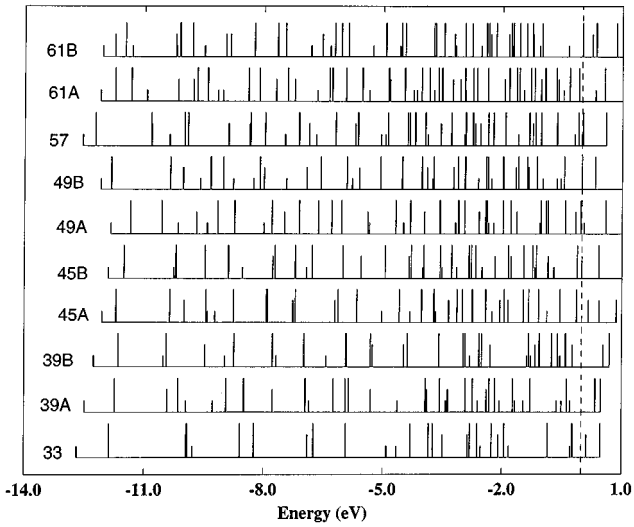

FIG. 9. Density of states of the different SRIG models (shifted on the vertical axis for clarity). The height of lines represents the degeneracy (1, 2, or 3). The vertical dashed line is the Fermi energy.

the cohesive energy of bulk Si, we have opted to quote the cohesive energy per atom of each cluster by comparing the cluster energy to an equivalent number of bulk Si atoms, and using the experimental value for the cohesive energy of the bulk (4.68 eV). In this way, the quoted energies per atom for the clusters should be closer to realistic cohesive energies. For the bulk calculation, we use the same plane-wave cutoff, the primitive two-atom unit cell of the diamond lattice, and a set of k points that produces a density in reciprocal space equivalent to the center of the supercell cube in the cluster calculations.

Table II contains a comparison of the cohesive energy per atom and the corresponding energy gap between the highest occupied molecular orbital (HOMO) and lowest unoccupied molecular orbital (LUMO), for the different clusters we studied. The model with the highest cohesive energy per atom (49A) has almost 82% of the bulk cohesive energy, while the model with the lowest cohesive energy (39B) has 77% of the bulk cohesive energy. Figure 9 shows the density of states (DOS) for each model. The symmetry of the clusters dictates that the electronic states are singly, doubly, or triply degenerate, according to the dimensions of the irreducible representations of the tetrahedral group. In all cases the total bandwidth (between 12 and 13 eV) is comparable to that of the bulk.

There are some interesting insights revealed by these comparisons of cohesive energies and electronic structure. The cluster with the smallest cohesive energy (least stable energetically) is the cluster with 39 atoms and trimer units at the tetrahedron surfaces (model 39B, Fig. 3). The relatively high energy of this cluster can be rationalized as being due to the strain induced by the trimer units. Interestingly, this cluster also has the largest HOMO-LUMO gap. Thus, at least for the structures considered here, there is no direct correlation between the energetic stability and the HOMO-LUMO gap. The existence of a large HOMO-LUMO gap may be indicative of low chemical reactivity, since in this case the system has a closed electronic shell. In this sense, if the 39B SRIG model were to be formed, it might be expected to have low chemical reactivity. However, a quantitative study of chemical reactivity should involve a more detailed examination of cluster electronic states, as well as case studies of chemical reactions between the cluster and representative molecular agents.[46] The presence of a different model of the same size (39A) that has lower energy and a comparable HOMO-LUMO gap suggests that the likelihood of the geometry 39B being realized is small.

Another interesting point is that the lowest-energy clusters are the two models with 49 atoms, closely followed by the 45A model and the 33 model. While the 45A and 33 models have significant HOMO-LUMO gaps, the two 49-atom models have very small (49A) or nonexistent (49B) gaps. Thus, based on the simple arguments mentioned above on the relation of the HOMO-LUMO gap to chemical reactivity, one might expect that the models 33 and 45A will exhibit low chemical reactivity, while models 49A and 49B will have higher chemical reactivity, despite their lower energy per atom. This is consistent with the experimental findings of Jarrold and Honea,[47] who observed that chemical reactivity and thermodynamic stability are not related. Finally, the larger clusters of sizes 57 and 61 again have very small (57) or nonexistent (61A,61B) gaps, suggesting high chemical reactivity despite their relative energetic stability (especially for model 61A).

IV. DISCUSSION AND CONCLUSIONS

We have presented a detailed discussion of the geometric features, the relative energies, and the electronic structure of models for Si clusters of sizes 33, 39, 45, 57, and 61. The basic characteristic of these models is their resemblance to bulk Si, including geometries of the exterior atoms that resemble surface reconstruction features and geometries of the interior atoms that resemble the fourfold tetrahedral coordination of the bulk. Although this is an appealing feature, it does not guarantee that these models are the energetically preferred geometries. In fact, it seems that molecular dynamics (MD) or simulated annealing (SA) simulations based on empirical,[48] semiempirical,[49] and first-principles calculations[50,51] tend to give geometries different from the ones proposed here. Therefore, it is important to address to what extent the models considered here are relevant to the structure of real Si clusters.

We suggest that these models may indeed be relevant to the structure of real Si clusters for the following reasons.

(1) It appears from experiment that there is something special about the chemical reactivity of the (so-called ''magic'') sizes 33, 39, and 45, while other clusters have approximately constant and much higher (by several orders of magnitude) reactivity from these magic numbers.[25–28,30] It is appealing that for all the magic number sizes we were able to construct SRIG models, and that these particular models have the largest HOMO-LUMO gaps of all the structures considered. Moreover, the SRIG models of sizes 49, 57, and 61, which are energetically equally stable stable as the magic numbers, have very small or nonexistent HOMO-LUMO gaps. In this sense, the pattern of SRIG models is compatible with the pattern of experimental measurements of reactivity,

assuming that the HOMO-LUMO gap can be used as a coarse measure of chemical reactivity (with the caveats mentioned in Sec. III).

(2) If the clusters of various sizes possess no special geometric features, as the simulations based on various methodologies suggest,[48–51] then it is difficult to explain the dramatic changes in reactivity and the existence of the magic numbers. Actually, MD simulations based on DFT-LDA (Ref. 50) reported that by augmenting by one atom the core of their optimal 45-atom geometry consisting of a 38-atom outer shell and a 7-atom core, a cluster of 46 Si atoms is obtained that has the same cohesive energy, the same outer shell, and the same number of ''dangling bonds'' as the original 45-atom model. In other words, adding one atom to the 45-atom model gives a cluster of the same stability (cohesive energy), surface structure (outer shell), and electronic states (number of dangling bonds). Consequently, the reactivity of the 45- and 46-atom clusters obtained by these simulations should be essentially identical, in direct contradiction to experiment.[25–28,30] The SRIG models presented here give a natural explanation to this problem: since the SRIG models (e.g., the 45-atom model with the lowest energy) correspond to a perfectly reconstructed outer shell, the addition or subtraction of one atom will drastically change the structure because it cannot be accommodated as part of the outer shell reconstruction or of the interior, and thus the reactivity of the cluster will be significantly increased.

(3) The methodologies employed to search for possible cluster structures in MD or SA simulations have limitations, especially when it comes to comparing geometries that are very different in bonding arrangements. This applies to the empirical and semiempirical methodologies, but also to a certain extent to the DFT-LDA methodologies. It has been argued, for example, that electron correlation effects are crucial in stabilizing the structure of certain Si clusters,[52,53] while such effects are not explicitly included in the DFT-LDA simulations.[50,51] In the present work, we have used the DFT-LDA approach *only for optimization of the structure* of models within the proposed very strict geometric constraints, that is, as if the overall structure of the cluster were known. It is well established that this methodology gives reasonable agreement with experiment for the detailed structural features (i.e., bond lengths and bond angles) of molecules, when the overall geometry is known. The electronic structure corresponding to a known geometry is also reasonably well obtained. There are, however, examples where this methodology has proven inadequate in comparing the energetics of very different structures for a cluster of a given size and composition, for instance, the cases where strong correlation effects are present.[52,53] In this sense, it may be overly optimistic to rely on DFT-LDA simulations in order to determine the structure of Si clusters in the size range considered here, without imposing any geometric constraints. If this is true, the results of empirical or semiempirical simulations could be even less reliable, as far as unconstrained structure optimization of specific cluster sizes is concerned.

(4) Even if a methodology that is very accurate were available, the task of determining the optimal structure of clusters in this size range is daunting. The review of Jones and Gunnarson[54] presents persuasive arguments on the intractability of finding the global energy minimum for a structure with several tens of atoms through an unguided search over configurational space. In fact, it is very likely that the structures with special properties (such as the magic numbers) correspond to deep and narrow wells in the multidimensional configurational space, which are difficult to locate by unguided searches. What we have provided here are physically motivated models that could potentially correspond to such deep and narrow wells in the energy landscape. The proper approach would then be to use such models as starting points for searches of the configurational space. Even in this case, extreme caution should be used in performing simulations, since it is relatively easy to bring the structure outside the well if the bottom has not been reached by thorough relaxation. As an example, in the present work we have found that the cluster geometry can be stuck in local energy minima and is prevented from reaching the bottom of the energy well, simply due to the initial occupation of the electronic states. For this reason, the number of electronic states used in a DFT-LDA simulation must exceed the number of states required to accommodate the electrons, and the filling of the states near the Fermi level must be varied in order to achieve good relaxation and to avoid getting trapped in local energy minima. Once outside the minimum-energy well, the simulation may end up exploring irrelevant and uninteresting structures which correspond to broad shallow basins in the energy landscape.

In conclusion, we have discussed a set of models for Si clusters in the range 33–61 atoms, which are physically motivated and exhibit interesting patterns in their energy and electronic structure. These models may be relevant to understanding the exceptionally low chemical reactivity of certain magic number sizes. The pattern of HOMO-LUMO gaps exhibited by these models is consistent with the magic number clusters of low reactivity. Finally, the models are compact clusters with little concave surface area, and the lowest energy ones tend to have small cross sections. The models 33, 39B, 45A, and 49B are in excellent agreement with the recent innovative experiments of Jarrold and co-workers on the gas phase mobility of Si clusters,[42,45] suggesting that these models may be relevant to the actual structure of Si clusters.

ACKNOWLEDGMENTS

This work was performed during the Worskshop on Quantitative Methods in Materials Research at ITP, supported by the National Science Foundation under Grant No. PHY94-07194. The author is indebted to A. A. Shvartsburg and M. F. Jarrold for providing the results of their mobility calculations for selected Si clusters and for sharing experimental results prior to publication.

*On leave from Physics Department and Division of Engineering and Applied Sciences, Harvard University, Cambridge, MA 02138.

[1] See for example, L. Brus, J. Chem. Phys. **98**, 3575 (1994); *Proceedings of NATO Advanced Study Institute, School on Nanophase Materials,* edited by G. C. Hadjipanayis (Kluwer

Academic, Dordrecht, 1993); Adv. Mater. **5**, 286 (1993).
[2] J. C. Phillips, J. Chem. Phys. **85**, 5246 (1986); **87**, 1712 (1987); **88**, 2090 (1988).
[3] L. A. Bloomfield, R. R. Freeman, and W. L. Brown, Phys. Rev. Lett. **54**, 2246 (1985).
[4] Y. Liu, Q.-L. Zhang, F. K. Tittel, R. F. Carl, and R. E. Smalley, J. Chem. Phys. **85**, 7434 (1986).
[5] J. R. Chelikowsky, Phys. Rev. Lett. **60**, 2669 (1988).
[6] D. Tomanek and M. A. Schlüter, Phys. Rev. Lett. **56**, 1055 (1986); Phys. Rev. B **36**, 1208 (1987).
[7] M. F. Jarrold, Science **252**, 1085 (1991); M. F. Jarrold and V. A. Constant, Phys. Rev. Lett. **67**, 2994 (1991); M. F. Jarrold and J. E. Bower, J. Chem. Phys. **96**, 9180 (1992).
[8] E. Kaxiras and K. Jackson, Phys. Rev. Lett. **71**, 727 (1988).
[9] J. R. Chelikowsky, J. C. Phillips, M. Kamal, and M. Strauss, Phys. Rev. Lett. **62**, 292 (1989); J. R. Chelikowsky, K. Glassford, and J. C. Phillips, Phys. Rev. B **44**, 1538 (1991).
[10] K. Raghavachari, J. Chem. Phys. **84**, 5672 (1986); K. Raghavachari and C. M. Rohlfing, *ibid.* **89**, 2219 (1988); K. Raghavachari and C. M. Rohlfing, Chem. Phys. Lett. **198**, 521 (1992).
[11] P. Ballone, W. Andreoni, R. Car, and M. Parrinello, Phys. Rev. Lett. **60**, 271 (1988); W. Andreoni and G. Pastore, Phys. Rev. B **41**, 10 243 (1990); U. Röthlisberger, W. Andreoni, and P. Gianozzi, J. Chem. Phys. **96**, 1248 (1992).
[12] N. Binggeli, J. L. Martins, and J. R. Chelikowsky, Phys. Rev. Lett. **68**, 2956 (1992); N. Binggeli and J. R. Chelikowsky, Phys. Rev. B **50**, 11 764 (1994); X. Jing, N. Troullier, D. Dean, N. Binggeli, and J. R. Chelikowsky, *ibid.* **50**, 12 234 (1994).
[13] E. C. Honea, A. Ogura, C. A. Murray, K. Raghavachari, W. O. Sprenger, M. F. Jarrold, and W. L. Brown, Nature (London) **366**, 42 (1993).
[14] L. A. Curtiss, P. W. Deutsch, and K. Raghavachari, J. Chem. Phys. **96**, 6868 (1992); C. M. Rohlfing and K. Raghavachari, *ibid.* **96**, 2114 (1992).
[15] S. Li, R. J. Van Zee, W. Weltner, and K. Raghavachari, Chem. Phys. Lett. **243**, 275 (1995).
[16] X. Jing *et al.*, Solid State Commun. **96**, 231 (1995).
[17] N. Binggeli and J. R. Chelikowsky, Phys. Rev. Lett. **75**, 493 (1995).
[18] S. Nagase and K. Kobayashi, Chem. Phys. Lett. **187**, 291 (1991); S. Nagase, Pure Appl. Chem. **65**, 675 (1993); S. Nagase and K. Kobayashi, Fullerene Sci. Technol. **1**, 299 (1993); K. Kobayashi and S. Nagase, Bull. Chem. Soc. Jpn. **66**, 3334 (1993).
[19] M. Menon and K. R. Subbaswamy, Chem. Phys. Lett. **219**, 219 (1994).
[20] J. C. Grossman and L. Mitas, Phys. Rev. B **52**, 16 735 (1995).
[21] A. Bahel, J. Pan, and M. V. Ramakrishna, Mod. Phys. Lett. B **9**, 811 (1995); A. Bahel and M. V. Ramakrishna, Phys. Rev. B **51**, 13 849 (1995); M. V. Ramakrishna and A. Bahel, J. Chem. Phys. **104**, 9833 (1996).
[22] E. Kaxiras, Chem. Phys. Lett. **163**, 323 (1989); Phys. Rev. Lett. **64**, 551 (1990).
[23] C. H. Patterson and R. P. Messmer, Phys. Rev. B **42**, 7530 (1990).
[24] J. Pan and M. V. Ramakrishna, Phys. Rev. B **50**, 15 431 (1994).
[25] J. L. Elkind, J. M. Alford, F. D. Weiss, R. T. Laaksonen, and R. E. Smalley, J. Chem. Phys. **87**, 2397 (1987).
[26] U. Ray and M. F. Jarrold, J. Chem. Phys. **93**, 5709 (1990); M. F. Jarrold, Y. Ijiri, and U. Ray, *ibid.* **94**, 3607 (1991).
[27] M. F. Jarrold, J. E. Bower, and K. M. Creegan, J. Chem. Phys. **90**, 3615 (1989); L. R. Anderson, S. Maruyama, and R. E. Smalley, Chem. Phys. Lett. **176**, 348 (1991).
[28] M. F. Jarrold, U. Ray, and K. M. Creegan, J. Chem. Phys. **93**, 224 (1990); J. E. Bower and M. F. Jarrold, *ibid.* **97**, 8312 (1992).
[29] U. Ray and M. F. Jarrold, J. Chem. Phys. **94**, 2631 (1991).
[30] S. Maruyama, L. R. Anderson, and R. E. Smalley, J. Chem. Phys. **93**, 5349 (1990); J. M. Alford, R. T. Laaksonen, and R. E. Smalley, J. Chem. Phys. **94**, 2618 (1991).
[31] K. Takayangi, Y. Tanishiro, M. Takahashi, and S. Takahashi, J. Vac. Sci. Technol. A **3**, 1502 (1985); Surf. Sci. **164**, 367 (1985).
[32] G. Rosensteel and D. J. Rowe, Phys. Rev. Lett. **47**, 223 (1981).
[33] The structure of this cluster was first discussed by H. W. Kroto, Nature (London) **329**, 529 (1987).
[34] T. Guo, *et al.*, Science **257**, 1661 (1992).
[35] M. R. Pederson and N. Laouini, Phys. Rev. B **48**, 2733 (1993); B. I. Dunlap, O. D. Häberlen, and N. Rösch, J. Phys. Chem. **96**, 9095 (1992); O. D. Häberlen, N. Rösch, and B. I. Dunlap, Chem. Phys. Lett. **200**, 418 (1992); K. A. Jackson, E. Kaxiras, and M. R. Pederson, Phys. Rev. B **48**, 17 556 (1993).
[36] E. Kaxiras, Y. Bar-Yam, J. D. Joannopoulos, and K. C. Pandey, Phys. Rev. Lett. **57**, 106 (1986); D. K. Biegelsen, R. D. Bringans, J. E. Northrup, and L.-E. Swartz, *ibid.* **65**, 452 (1990).
[37] P. Martensson, G. Meyer, N. M. Amer, E. Kaxiras, and K. C. Pandey, Phys. Rev. B **42**, 7230 (1990).
[38] I.-S. Hwang and J. A. Golovchenko, Phys. Rev. B **50**, 18 535 (1994); I.-S. Hwang, R. E. Martinez, C. Liu, and J. A. Golovchenko, *ibid.* **51**, 10193-6 (1995); J. A. Golovchenko, I.-S. Hwang, C. Liu, and R. E. Martinez, Surf. Sci. **323**, 241 (1995).
[39] P. Hohenberg and W. Kohn, Phys. Rev. **136**, B864 (1964); W. Kohn and L. J. Sham, *ibid.* **140**, A1133 (1965).
[40] R. Car and M. Parrinello, Phys. Rev. Lett. **55**, 2471 (1985); R. Stumpf and M. Scheffler, Comput. Phys. Commun. **79**, 447 (1994).
[41] G. B. Bachelet, D. R. Hamann, and M. Schlüter, Phys. Rev. B **26**, 4199 (1982).
[42] P. Dugourd, R. R. Hudgins, D. E. Clemmer, and M. F. Jarrold, Rev. Sci. Instrum. **68**, 1122 (1997); M. F. Mesleh, J. M. Hunter, A. A. Shvartsburg, G. C. Schatz, and M. F. Jarrold, J. Phys. Chem. **100**, 16 082 (1996); *ibid.* **101A**, 968 (1997); A. A. Shvartsburg, R. R. Hudgins, P. Dugourd, and M. F. Jarrold, *ibid.* **101A**, 1684 (1997).
[43] A. A. Shvartsburg (private communication).
[44] A. A. Shvartsburg and M. F. Jarrold, Chem. Phys. Lett. **261**, 86 (1996).
[45] A. A. Shvartsburg and M. F. Jarrold (unpublished).
[46] M. V. Ramakrishna and J. Pan, J. Chem. Phys. **101**, 8108 (1994).
[47] M. F. Jarrold and E. C. Honea, J. Am. Chem. Soc. **114**, 459 (1992).
[48] B. L. Swift, D. A. Jelski, D. S. Higgs, T. T. Rantala, and T. F. George, Phys. Rev. Lett. **66**, 2686 (1991); D. A. Jelski, B. L. Swift, T. T. Rantala, X. Xia, and T. F. George, J. Chem. Phys. **95**, 8552 (1991).
[49] M. Menon and K. R. Subbaswamy, Phys. Rev. B **47**, 12 754 (1993); **51**, 17 952 (1995).
[50] U. Röthlisberger, W. Andreoni, and M. Parrinello, Phys. Rev. Lett. **72**, 665 (1994).
[51] S. Mukherjee, A. P. Scitsonen, and R. M. Nieminen, *Clusters and Nanostructured Materials*, edited by P. Jena and S. N. Behera (Nova Science, Commack, NY, 1996), pp. 165–171.
[52] J. C. Phillips, Phys. Rev. B **47**, 14 132 (1993).
[53] J. C. Grossman and L. Mitas, Phys. Rev. Lett. **74**, 1323 (1995).
[54] R. O. Jones and O. Gunnarson, Rev. Mod. Phys. **61**, 689 (1989).